High Frequency (139.5 GHz) Electron Paramagnetic Resonance Characterization of Mn(II)−$H_2{}^{17}O$ Interactions in GDP and GTP Forms of p21 *ras*†

Brendan F. Bellew,‡ Christopher J. Halkides,§,|| Gary J. Gerfen,‡ Robert G. Griffin,*,‡ and David J. Singel*,⊥

Department of Chemistry and Francis Bitter Magnet Laboratory, Massachusetts Institute of Technology, Cambridge, Massachusetts 02139, Department of Biochemistry, Brandeis University, Waltham, Massachusetts 02154, and Department of Chemistry and Biochemistry, Montana State University, Bozeman, Montana 59717

Received March 11, 1996; Revised Manuscript Received July 9, 1996⊗

ABSTRACT: As a molecular switch, the *ras* protein p21 undergoes structural changes that couple recognition sites on the protein surface to the guanine nucleotide−divalent metal ion binding site. X-ray crystallographic studies of p21 suggest that coordination between threonine-35 and the divalent metal ion plays an important role in these conformational changes. Recent ESEEM studies of p21 in solution, however, place threonine-35 more distant from the metal and were interpreted as weak or indirect coordination of this residue. We report high frequency (139.5 GHz) EPR spectroscopy of p21·Mn(II) complexes of two guanine nucleotides that probes the link between threonine-35 and the divalent metal ion. By analysis of high-frequency EPR spectra, we determine the number of water molecules in the first coordination sphere of the manganous ion to be four in p21·Mn(II)·GDP, consistent with prior low-frequency EPR and X-ray crystallographic studies. In the complex of p21 with a GTP analog, p21·Mn(II)·GMPPNP, we determine the hydration number to be 2, also consistent with crystal structures. This result rules out indirect coordination of threonine-35 in the solution structure of p21·Mn(II)·GMPPNP, and implicates direct, weak coordination of this residue as suggested by Halkides et al. [(1994) *Biochemistry 33*, 4019]. The ^{17}O hyperfine coupling constant of $H_2{}^{17}O$ is determined as 0.25 mT in the GDP form and 0.28 mT in the GTP form. These values are similar to reported values for ^{17}O-enriched aquo ligands and some phosphato ligands in Mn(II) complexes. The high magnetic field strength (4.9 T) employed in these 139.5 GHz EPR measurements leads to a narrowing of the Mn(II) EPR lines that facilitates the determination of ^{17}O hyperfine interactions.

The protein *ras* p21[1] (hereafter referred to as p21) belongs to the important family of homologous GTP-hydrolyzing proteins, which also includes elongation factors (exemplified by EF-Tu) and the α subunits of heterotrimeric G proteins (Bourne et al., 1990) among its widely-studied members. p21 transduces and amplifies signals regulating cell growth and differentiation (Bourne et al., 1991). p21 cycles between two forms, binding, alternately, the divalent metal ion complexes of GTP or GDP (Milburn et al., 1990). Interactions of p21 with other proteins in the signaling pathway regulate the cycling between the two forms. Likewise, p21 transmits a signal for cell growth or differentiation through binding to its principal downstream effector, Raf-1 (Shirouzu et al., 1994). The GTP form of p21 transduces the signals promoting cell growth or differentiation, while the GDP form does not (Moodie et al., 1993). Certain point mutations in the *ras* gene and the resultant oncoproteins have been implicated in numerous human tumors (Barbacid, 1987; Downward, 1990). These oncoproteins tend to remain in the GTP-bound form for prolonged periods and thus overstimulate cell growth (Milburn et al., 1990).

The crystal structures of p21·Mg(II) complexes of GDP (Milburn et al., 1990; Schlichting et al., 1990; Tong et al., 1991), GTP (Schlichting et al., 1990), GMPPCP (Milburn et al., 1990), and GMPPNP (Pai et al., 1990) have been examined by X-ray diffraction. These studies suggest that the function of p21 as a molecular switch is linked to conformational differences between the GDP form and GTP form of p21. The conformational changes at the nucleotide binding site are apparently coupled to two highly exposed sites on the protein surface. These sites, which are part of the Switch I (amino acid residues 30−38) and Switch II (residues 60−76) regions, are also part of the recognition sites for proteins which bind p21 (Marshall, 1993). In order to study a protein whose function is modulated by protein−protein interactions, it is desirable to augment crystallographic studies, in which the structure may be altered by

† Supported by NIH Grant GM-38352 (R.G.G. and D.J.S.). Supported by USPHS Grant 7UI01 CA51992 to Onyx Corp. and NIH Grant 5R 37 GM20168. C.J.H. was supported by NIH Postdoctoral Fellowship CA-08872. G.J.G. was supported by Postdoctoral Fellowships from NIH (GM-14404) and ACS (PF-3668).

* Authors to whom correspondence should be addressed.

‡ Massachusetts Institute of Technology.

§ Brandeis University.

|| Present address: Institute of Molecular Biology, University of Oregon, Eugene, OR 97404.

⊥ Montana State University at Bozeman.

⊗ Abstract published in *Advance ACS Abstracts,* August 15, 1996.

[1] Abbreviations: *ras*, the *ras* gene; p21, product of the *ras* gene; N, neuroblastoma; H, Harvey; GAP, GTPase-activating protein; EF-Tu, elongation factor Tu; EPR, electron paramagnetic resonance; ESEEM, electron spin-echo envelope modulation; NMR, nuclear magnetic resonance; ENDOR, electron−nuclear double resonance; GDP, guanosine 5′-diphosphate; GTP, guanosine 5′-triphosphate; GMPPNP, guanosine 5′-(β,γ-imidotriphosphate); GMPPCP, guanosine 5′-(β,γ-methylenetriphosphate); α_1, the first α-helix of p21 (residues 15−26); α_2, the second α-helix of p21 (residues 67−75); λ_1, the first loop of p21 (residues 10−14); λ_2, the second loop of p21 (residues 27−37); λ_4, the fourth loop of p21 (residues 59−66); P_i, inorganic phosphate; ADP, adenosine 5′-diphosphate; ATP, adenosine 5′-triphosphate; $p21_c$, cellular H-*ras* p21 containing Gly-12 and Ala-59; $p21_t$, T24 mutant form containing Val-12; $p21_v$, viral H-*ras* p21 containing Arg-12 and Thr-59; AK, adenylate kinase; CK, creatine kinase; PK, pyruvate kinase; Thr-35, threonine-35.

S0006-2960(96)00594-6 CCC: $12.00

interactions between p21 molecules in the crystal (Foley et al., 1992), with studies of the isolated protein in solution. Recently, we initiated a series of experiments, using EPR spectroscopy in conjunction with isotopic labeling, designed to probe the nucleotide binding site structure of p21 in solution.

GDP and GMPPNP complexes of p21·Mn(II) were studied by ESEEM in frozen solution (Halkides et al., 1994; Larsen et al., 1992). Initially (Larsen et al., 1992), selectively labeled (^{15}N) and natural abundance (^{31}P and ^{1}H) nuclei of the amino acids glycine and serine, and of the nucleotide GDP, were examined. This work was subsequently extended to include all of the putative ligands of the divalent metal by selectively labeling (^{13}C, ^{15}N, and ^{2}H) the amino acids serine, glycine, aspartate, and threonine, and by utilizing the natural abundance of ^{31}P nuclei to study the nucleotides GDP and GMPPNP (Halkides et al., 1994). These ESEEM studies yield the distances between the manganous ion and the labeled nuclei of the amino acids and nucleotides; coordination of the manganous ion by the amino acids and nucleotides is inferred from the measured distances and from the presence of contact hyperfine interactions.

The ESEEM studies of p21 have yielded structural results in general accord with those derived from X-ray crystallography regarding the relation of the divalent metal ion to the Switch I (λ_2) and Switch II (λ_4 and α_2) regions, and to the phosphate binding region (λ_1 and α_1) in the GDP form; likewise, in the GTP form, there is general accord regarding its relation to the Switch II and phosphate binding regions. An intriguing difference, however, is found in the Switch I region.

X-ray crystallographic studies show threonine-35 to be a ligand in the GTP form, but not in the GDP form. The binding of threonine-35 has accordingly been alleged to drive the pivotal change in the conformation of the Switch I domain that distinguishes the growth-active and quiescent forms of p21 (Marshall, 1993). ESEEM measurements consistently show that the distance between the manganous ion and the hydroxyl oxygen of threonine-35 must be greater than the canonical distance (~2.2 Å) of first sphere oxygen−manganous ion coordination (Halkides et al., 1994). The difference between the crystal structure and the ESEEM results is likely to be an effect of crystal packing: the interprotein contacts near threonine-35 could perturb the protein structure in this region. In addition, Switch I and, particularly, Switch II show greater than average disorder (Milburn et al., 1990; Pai et al., 1990) in the crystal structures. The ESEEM observations allow two interpretations regarding metal coordination in solution: either threonine-35 coordinates the manganous ion directly but weakly or threonine-35 coordinates indirectly *via* a water molecule (Halkides et al., 1994).

In order to clarify the nature of the coordination of threonine-35, we undertook an EPR investigation of the hydration of the manganous ion in p21. Since the coordination number of the manganous ion is, with rare exception, six, the measurement of the hydration number also determines the number of non-aquo ligands. Thus, in view of the coordination of serine-17 and the β- and γ-phosphates in the GTP form (Milburn et al., 1990; Pai et al., 1990), the expected hydration number is 2 if threonine-35 coordinates directly; if it coordinates *via* a water molecule, the expected hydration number is 3.

Reed and co-workers developed a useful scheme for measuring manganous ion hydration numbers by EPR. The method relies on the detection of hyperfine broadening from ^{17}O-enriched aquo ligands within the relatively sharp Mn(II) EPR central fine structure transition.[2] ^{17}O hyperfine broadening competes against other sources of broadening—primarily unresolved ^{1}H and ^{31}P hyperfine interactions and second-order fine structure broadening. Since the contribution of second-order fine structure broadening[2] is *inversely* proportional to B_0, whereas hyperfine broadening is field-independent, the latter is accentuated at higher magnetic field strengths. EPR of Mn(II) complexes with ^{17}O labeling is therefore often done at 35 GHz rather than at the more conventional frequency, 9 GHz (Buchbinder & Reed, 1990; Feuerstein et al., 1987; Kalbitzer et al., 1984, 1983; Kofron et al., 1992; Latwesen et al., 1992; Leyh et al., 1982; Lodato & Reed, 1987; Moore & Reed, 1985; Olsen & Reed, 1993; Reed & Leyh, 1980; Smithers et al., 1990; Wittinghofer et al., 1982). Nevertheless, even at 35 GHz, fine structure interactions can mask ^{17}O hyperfine couplings. A number of systems, including p21·Mn(II)·GTP analog complexes ($D \approx 20$ mT) and EF-Tu·Mn(II)·GTP analog complexes, appear to have zero-field splitting parameters so large that EPR measurements of hydration numbers could not be carried out at 35 GHz. The D^2/B_0 dependence of the fine structure broadening, however, leads to the prediction that ^{17}O hyperfine broadening could be observed in EPR spectra of a p21·Mn(II)·GTP analog complex at 140 GHz. The experiments reported here provide the first determination of the hydration number of a p21·Mn(II)·GTP analog complex.

MATERIALS AND METHODS

Samples. Cloning, overexpression, and purification of the H- and N-*ras* p21 proteins as well as preparation of p21 complexes of Mn(II)·GDP and Mn(II)·GMPPNP were performed as described previously (Halkides et al., 1994), with the exception that protein solutions were prepared with 0.01% (w/v) *n*-octyl β-glucopyranoside. Two aliquots, each ~6 μL, were taken from the protein solution (~1 mM). Approximately 200 nL of the first aliquot was transferred by capillary action to a fused silica sample tube with id 0.40 mm and od 0.55 mm (Wilmad), which was then sealed with silicone high vacuum grease (Dow Corning). The second aliquot was lyophilized and subsequently rehydrated to its original volume with 30% ^{17}O-enriched water (Cambridge Isotope Laboratories). A portion of this sample was transferred to and sealed into a sample tube.

EPR Spectroscopy. EPR measurements were made at 139.500 GHz with a super-heterodyne spectrometer designed and fabricated in this laboratory and described elsewhere (Becerra et al., 1995; Prisner et al., 1992). The external

[2] At high fields ($B_0 \gg D$, where D is the zero-field splitting parameter and B_0 is the magnitude of the external magnetic field), only $\Delta M_S = \pm 1$ transitions make a significant contribution to the EPR signal of Mn(II) (electron spin $S = {}^5/_2$, Mn nuclear spin $I = {}^5/_2$) (Reed & Markham, 1984). In orientationally disordered samples, the zero-field splitting (also referred to as the fine structure interaction) broadens the $M_S = \pm{}^5/_2 \rightleftharpoons \pm{}^3/_2$ and $M_S = \pm{}^3/_2 \rightleftharpoons \pm{}^1/_2$ transitions by $5D$ and $3D$ respectively. The fine structure interaction broadens the central fine structure transition ($M_S = -{}^1/_2 \rightleftharpoons +{}^1/_2$) by $\approx(55/9)D^2/B_0$ (Abragam & Bleaney, 1970). Thus the significantly narrower central fine structure transition dominates the EPR signal of manganous ions at high field. The central fine structure transition is typically split into a well-resolved hyperfine sextet by a hyperfine interaction with the ^{55}Mn nucleus.

magnetic field was modulated at a frequency of 400 Hz and an amplitude of 0.080 mT. Two lock-in amplifiers (E.G.&G. Princeton Applied Research, Model 5210) detect the resulting quadrature pair of modulated signals. The spectrometer is interfaced to a VAX workstation for data acquisition and processing.

A superconducting solenoid operating in the persistent mode generates the main field (4.95 T). The field is swept (±0.075 T, maximum) by varying the current in a concentric superconducting solenoid operating in the nonpersistent mode. A precision field sweep system, comprised of a deuterium NMR spectrometer and magnet power supply interfaced to the VAX workstation, measures and controls the magnetic field value (Un et al., 1989). In the determination of the manganous ion hydration number, B_0 is swept through the lowest-field (narrowest) member of the ^{55}Mn hyperfine sextet, from 4.9513 to 4.9620 T in 0.0250 mT increments.

Samples are contained within sample tubes positioned concentrically in a remotely-tuned, remotely-matched cylindrical TE_{011} mode resonator designed and built in this laboratory. Microwave power at the sample is approximately 20 μW, which corresponds to a B_1 field approximately equal to 0.01 mT. A steady flow of cold nitrogen gas over the resonator maintains the temperature at the sample within ±0.5 K of, typically, 180 K.

Each pair of quadrature-detected spectra was corrected for a base-line offset plus linear base-line drift. The quadrature-detected spectra were then phased to isolate the absorption and dispersion signals. For each sample, approximately 9−16 spectra were summed both to increase signal to noise ratios and to reduce phasing uncertainties (0.005π).

ANALYSIS

The Spectral Subtraction Method. In order to determine the number of H_2O molecules coordinated to the manganous ion (the hydration number), we employ the spectral subtraction method initially developed by Reed (Kofron et al., 1992; Latwesen et al., 1992; Lodato & Reed, 1987; Moore et al., 1985; Reed et al., 1980; Smithers et al., 1990). In a sample with a metal ion coordinated by n spectroscopically equivalent ^{17}O-enriched oxo ligands (with ^{17}O enrichment fraction equal to f_e), the experimentally acquired spectrum, S_e, can be viewed as a weighted sum of $n + 1$ conceptual subspectra, S_k, belonging to complexes with $k = 0, 1, ..., n$ ^{17}O ligands:

$$S_e = \sum_{k=0}^{n} w_k S_k \tag{1}$$

The fractional weighting coefficients, w_k, can be expressed as:

$$w_k = \frac{n!}{(n-k)!k!} f_e^{\,k} (1 - f_e)^{n-k} \tag{2}$$

and in particular,

$$w_0 = (1 - f_e)^n \tag{3}$$

Since ^{17}O has a natural abundance essentially equal to zero (0.037%), the experimentally acquired spectrum of a sample unenriched in ^{17}O, S_u, can be taken as identical to subspectrum S_0, which is the narrowest subspectrum (no ^{17}O broadening) of the composite spectrum. Now consider a difference spectrum, S_d, of the following form:

$$S_d = S_e - \kappa S_u \tag{4}$$

in which κ is an adjustable parameter between 0 and 1. This difference spectrum can be rewritten as:

$$S_d = (w_0 - \kappa) S_0 + \sum_{k=1}^{n} w_k S_k \tag{5}$$

in which the decomposition of S_e (eq 1) as well as the identity of S_u and S_0 have been invoked. If κ is less than w_0, S_d is a sum of all $n + 1$ subspectra with positive contributions for each, albeit with a reduced contribution from S_0. If κ is equal to w_0, S_d is a sum of only the n ^{17}O hyperfine broadened subspectra with no contribution from S_0. If κ is greater than w_0, S_d is a sum of all $n + 1$ subspectra, but with a negative (anti-phase) contribution from the unbroadened S_0. Since S_0 is relatively narrow, this subtraction yields a difference spectrum with extraneous features when the intrinsic linewidth is not so large as to overwhelm the ^{17}O hyperfine interaction.

The treatment of the EPR data requires that S_u and S_e be normalized with respect to each other. A pair of modulation-detected absorption signals is taken to be normalized when their respective double integrals are equal at the upper bound. From the pair of normalized spectra, a series of difference spectra, S_d, are calculated with parametric variation of κ, until we find the greatest κ that yields a difference spectrum without extraneous features and the least κ that yields a difference spectrum with extraneous features. The former is the best estimate of w_0, and the latter is an upper bound on its value. If w_0 is found to be essentially equal to $(1 - f_e)^n$, then the simplest interpretation is that the metal ion—at all sites within the sample—is coordinated by n spectroscopically equivalent ^{17}O-enriched oxo ligands. We find it convenient to initiate our analysis with a coarse variation of κ with values defined by $\kappa = (1 - f_e)^m$, m an integer. This procedure gives a hydration number under the assumption that there is a single coordination number applicable to all sites in the sample. This assumption is then scrutinized by a fine variation of κ in the appropriate neighborhood.

Note that the only assumption made in this analysis is that all of the ^{17}O-enriched oxo ligands being counted are spectroscopically equivalent. The spectral subtraction method does not require simulations and therefore does not rely on a determination of ^{17}O hyperfine coupling constants.

Magnitude of the ^{17}O Hyperfine Interaction. Beyond the application of the spectral subtraction method, we further characterize Mn(II) hydration by determining the size of the ^{17}O hyperfine interaction for the aquo ligands, using a method similar to that previously described (Kalbitzer et al., 1984; Reed et al., 1980). Inasmuch as the ^{17}O hyperfine splittings are typically unresolved, the coupling constant is determined by comparison of S_e with spectral simulations. Since S_u is, by definition, identical to a perfect simulation incorporating all magnetic interactions except the ^{17}O hyperfine interactions, we take S_u as a starting point and further simulate only the ^{17}O hyperfine interactions. S_u is numerically broadened by convolution with a lineshape that models the isotropic hyperfine interaction with n (as determined by the spectral subtraction method) equivalent oxo ligands of some known

^{17}O enrichment. Thus there is only one free parameter—the ^{17}O hyperfine coupling constant. This coupling constant is varied parametrically in order to calculate a series of numerically broadened spectra. Comparison of S_e with this series of spectra yields a lower and an upper bound for the magnitude of the actual ^{17}O hyperfine interaction. Interpolation is used to refine the determination.

Because the ^{17}O hyperfine coupling is manifest only as a broadening of the EPR spectra, the isotropic and anisotropic components of the interaction cannot be independently determined. Therefore, the small anisotropic component of the ^{17}O hyperfine coupling, which arises from dipolar and psuedo-dipolar interactions, is not explicitly modeled in this analysis. Anisotropic contributions are expected to be <20% of the isotropic coupling based on ^{17}O−Mn(II) ENDOR studies (Glotfelty, 1978; Tan et al., 1995, 1993). Effects of such small anisotropic couplings are likely to fall within the uncertainties assigned to the values obtained for the isotropic couplings. The small ^{17}O quadrupole coupling interaction (on the order of 0.02 mT) (Tan et al., 1995) is also neglected.

Simulations. As a check on results, all experimentally acquired spectra and difference spectra are compared with detailed simulations done on a VAX workstation. Fifteen polar angles are sampled at equal intervals from 0 to π. At each polar angle, a number of azimuthal angles between one and thirty (and roughly equal to 30 times the sine of the polar angle) were sampled at even intervals from 0 to 2π. In order to simulate the effects of D strain, the simulation also included a truncated Gaussian distribution of D, the zero-field splitting parameter; the variance of the distribution was assumed to be equal to one-half of the mean; D was allowed to take on values within one variance from the mean. The ^{55}Mn nuclear spin took on all possible values $M_I = \pm^5/_2$, $\pm^3/_2$, $\pm^1/_2$. The resonant field for the central fine structure transition ($M_S = -^1/_2 \rightleftharpoons +^1/_2$) was first calculated assuming isotropic electronic Zeeman, isotropic ^{55}Mn hyperfine, and scalar ^{17}O hyperfine interactions. The resonant field was then corrected to include the effect of second-order terms proportional to D^2/B_0 and A^2/B_0, and third-order terms proportional to AD^2/B_0^2, A^2D/B_0^2, and A^3/B_0^2, where A is the ^{55}Mn hyperfine coupling constant (Reed et al., 1984). The g value and ^{55}Mn hyperfine coupling constant were measured from the spectra. The value of D for p21·Mn(II)·GDP was taken from Smithers et al. (1990); the value of D for p21·Mn(II)·GMPPNP was reported to us by George Reed (personal communication). The resulting distribution of resonant field values was convolved with Gaussian absorption and dispersion first-derivative lineshapes. The width of the lineshapes was determined by varying the width parametrically until there was good agreement between a simulated spectrum and S_u.

RESULTS AND DISCUSSION

Before illustrating specific applications of the spectral subtraction method, it is instructive to contrast the linewidths in 10 and 140 GHz Mn(II) EPR spectra. For this purpose, typical EPR signals of N-*ras* p21·Mn(II)·GMPPNP acquired at 9.755 GHz (top) and H-*ras* p21·Mn(II)·GMPPNP acquired at 139.5 GHz (bottom) are shown in Figure 1. The spectra are dominated by the central fine structure transition, which is split into a well-resolved sextet by the ^{55}Mn hyperfine interaction (~9.0 mT). The peak-to-peak linewidths of the individual sextet members are less than 1.0 mT at 140 GHz, but at 10 GHz the linewidths vary from 2.0 to 6.0 mT. This variation of linewidths across the sextet at 10 GHz arises from an additional term, proportional to $M_I D^2 A/B_0^2$, in the perturbative expression for the fine structure induced linewidth (Abragam & Bleaney, 1970). Clearly, the fine structure interaction plays a significant role in broadening the 10 GHz EPR spectrum. This broadening would make it relatively difficult to quantify ^{17}O hyperfine interactions at that frequency.

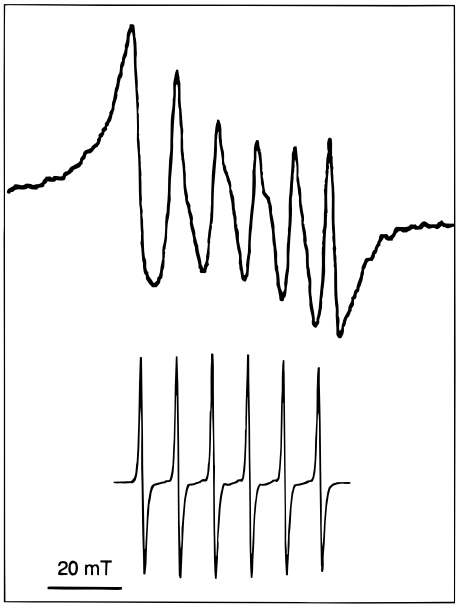

FIGURE 1: EPR spectra of frozen solutions of (top) N-*ras* p21·Mn(II)·GMPPNP acquired at 9.755 GHz and 4.2 K and (bottom) H-*ras* p21·Mn(II)·GMPPNP acquired at 139.5 GHz and 181 K.

GDP Form of p21. In order to facilitate comparison with the ESEEM results of Halkides et al. (1994), we made EPR measurements on frozen solutions under identical conditions of cryoprotection. In addition, we examined solutions frozen without cryoprotection. The effect of cryoprotection upon the Mn(II) EPR linewidth in the p21·Mn(II)·GDP complex is illustrated in Figure 2. The lowest-field member of the ^{55}Mn hyperfine sextet of the central fine structure EPR transition is shown. The spectrum labeled B is an EPR signal of p21·Mn(II)·GDP in frozen aqueous solution containing 15% (w/v) of the cryoprotectant methyl α-D-glucopyranoside. The spectrum labeled A is an EPR signal of the same complex in frozen aqueous solution without cryoprotection. The peak-to-peak linewidths of spectra A and B are 0.85 and 0.63 mT, respectively. As is commonly observed in EPR spectroscopy, the spectrum of the sample frozen without cryoprotection is significantly broader than that of the same sample frozen with cryoprotection.

In order to verify that addition of the cryoprotectant does not affect the hydration, we applied the spectral subtraction method to samples frozen with and without cryoprotection. The application to N-*ras* p21·Mn(II)·GDP frozen without (left) and with (right) 15% methyl α-D-glucopyranoside is illustrated in Figure 3.

Spectra A and B in Figure 3 are experimentally acquired EPR signals of N-*ras* p21·Mn(II)·GDP in frozen solutions of natural abundance and 30% ^{17}O-enriched water, respec-

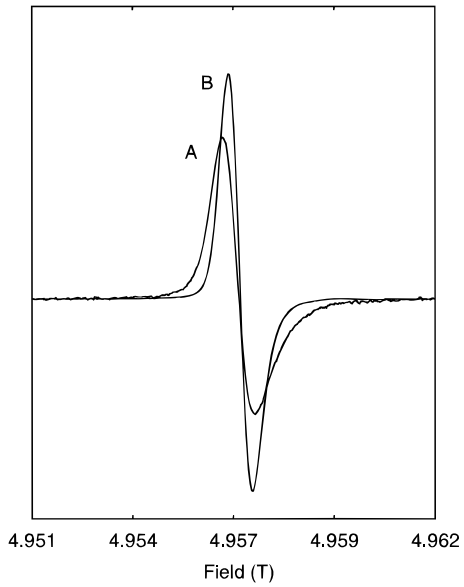

FIGURE 2: EPR spectra of N-*ras* p21·Mn(II)·GDP in frozen solutions (A) with no cryoprotectant and (B) with 15% (w/v) methyl α-D-glucopyranoside. Experimental parameters: microwave frequency, 139.5 GHz; temperature, ~180 K; modulation amplitude, 76.5 μT; modulation frequency, 0.400 kHz; B_1, ~3 μT.

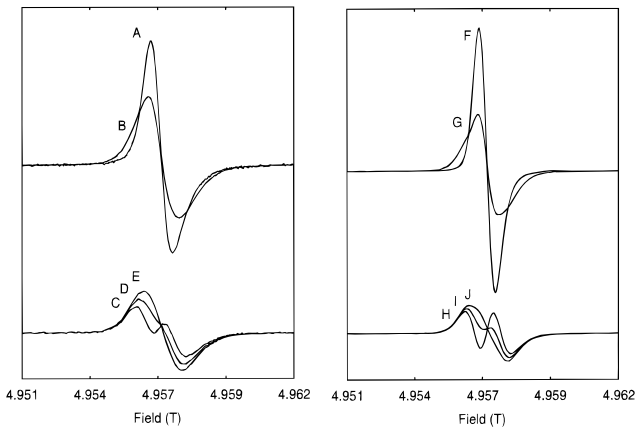

FIGURE 3: (Upper Left) Overlying EPR spectra of N-*ras* p21·Mn(II)·GDP in frozen solutions with no cryoprotectant and (A) unenriched water and (B) 30% ^{17}O-enriched water. (Lower Left) Overlying difference spectra calculated with (C) $\kappa = 0.70^2$, (D) $\kappa = 0.70^3$, and (E) $\kappa = 0.70^4$. The pair of local extrema appearing in (C), the pair of thin shoulders appearing in (D), and the absence of any extraneous features in (E) show that there are four waters in the first coordination sphere. (Upper Right) Overlying EPR spectra of N-*ras* p21·Mn(II)·GDP in frozen solutions with 15% methyl α-D-glucopyranoside and (F) unenriched water and (G) 30% ^{17}O-enriched water. (Lower Right) Overlying difference spectra calculated with (H) $\kappa = 0.70^2$, (I) $\kappa = 0.70^3$, and (J) $\kappa = 0.70^4$. The pairs of local extrema appearing in (H) and (I), but not (J), show that there are four waters in the first coordination sphere.

tively (no cryoprotection). Additional broadening, evidently from the ^{17}O hyperfine interaction, is clearly discernible in the spectrum of the enriched sample. Traces C, D, and E are difference spectra calculated by subtracting various fractions (κ) of spectrum A from spectrum B. The fractions were selected such that $\kappa = (1 - f_e)^m$, with m equal to 2, 3, and 4 for traces C, D, and E, respectively. (With 30% enrichment $1 - f_e = 0.70$.) An extraneous pair of local extrema appears in trace C, and a subtle but discernible pair of thin shoulders appears near the center of trace D, while no extraneous features appear in trace E. As explained in our discussion of the spectral subtraction method (*vide supra*), the best interpretation of this result is that the first coordination sphere contains four water molecules.

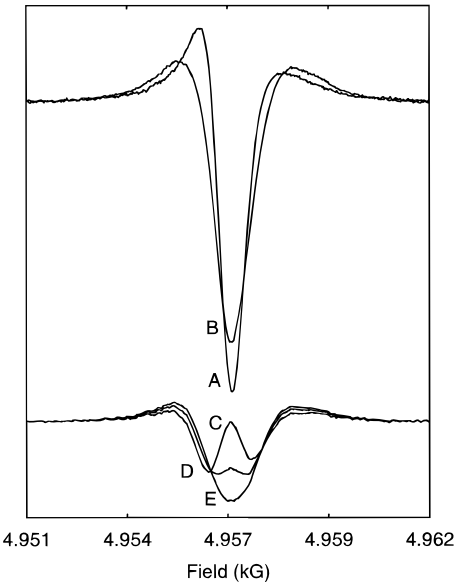

FIGURE 4: (Upper) Overlying dispersion mode EPR spectra of N-*ras* p21·Mn(II)·GDP in frozen solutions with no cryoprotectant and (A) unenriched water and (B) 30% ^{17}O-enriched water. (Lower) Overlying difference spectra calculated with (C) $\kappa = 0.70^2$, (D) $\kappa = 0.70^3$, and (E) $\kappa = 0.70^4$. The local maximum appearing in (C) and (D), but not (E), shows that there are four waters in the first coordination sphere.

Spectra F and G are EPR signals of N-*ras* p21·Mn(II)·GDP in cryoprotected (15% methyl α-D-glucopyranoside) frozen solutions of natural abundance and 30% ^{17}O-enriched water, respectively. Traces H, I, and J are difference spectra calculated with the same fractions (κ) as for traces C, D, and E. The pair of local extrema appearing in traces H and I, but not trace J, together with other calculated difference spectra (not shown) lead to the conclusion that the hydration number is four, as in the unprotected sample. Note that the reduction of the EPR linewidth in the presence of the cryoprotectant leads to a more pronounced effect of ^{17}O hyperfine interaction as can be appreciated by comparison of traces I and D in Figure 3.

Since the extraneous features in trace D are subtle, we further analyze non-cryoprotected samples by dispersion mode spectroscopy as illustrated in Figure 4. Spectra A and B in Figure 4 are the dispersion mode EPR signals of N-*ras* p21·Mn(II)·GDP in frozen solutions of natural abundance and 30% ^{17}O-enriched water, respectively (no cryoprotection). Traces C, D, and E are difference spectra calculated by subtracting the same three canonical fractions (κ) of trace A from trace B, with κ equal to 0.70^2, 0.70^3, and 0.70^4 for traces C, D, and E, respectively. The local maximum appearing in traces C and D, but not trace E, confirms that the hydration number is four.

Comparison of traces D in Figures 3 and 4 demonstrates the advantage of applying the spectral subtraction method to dispersion mode spectra for these relatively broad lines. In the absorption mode (Figure 3), the extra feature in trace D is merely a pair of thin shoulders, whereas in the dispersion mode (Figure 4), the extra feature in trace D is a distinct local maximum. The potentially subtle features introduced through the subtraction method are better evidenced in dispersion-mode rather than absorption-mode spectra: in the

former case, the difference features occur in an otherwise stationary spectral region, near the intensity maximum; in the latter, they occur in the region of greatest curvature, near the zero-crossing.

The hydration number that we determine for N-*ras* p21·Mn(II)·GDP is in complete agreement with the analogous results of an EPR study of H-*ras* p21·Mn(II)·GDP in fluid solution by Smithers et al. (1990) and Latwesen et al. (1992) at 35 GHz. This agreement demonstrates the validity of the spectral subtraction method in frozen solution notwithstanding the slight anisotropy of ^{17}O hyperfine interaction of aquo ligands in manganous ion complexes (Glotfelty, 1978). We find the principal advantage of working with frozen solutions is the achievement of higher signal-to-noise ratios, not only because lower temperatures yield increased Boltzmann factors, but also because of the possibility of admitting larger sample volumes without degrading the EPR resonator quality factor. Note that studies performed by us and by others (Smithers et al., 1990) indicate that freezing/lyophilization does not affect the GTPase activity of the thawed/rehydrated protein. The principal effect of cryoprotection is to reduce the EPR linewidth. This linewidth reduction enhances sensitivity to ^{17}O hyperfine broadening and facilitates the determination of hydration numbers by EPR spectroscopy. We also observe directly that the hydration number is unaffected by the introduction of 15% methyl α-D-glucopyranoside. ESEEM results give corroborating evidence that this particular cryoprotectant does not displace any aquo ligands from the first coordination sphere, but show that the more widely used cryoprotectant, glycerol, can, at high concentrations, substitute for waters in the first coordination sphere (Halkides et al., submitted).

A hydration number of four is completely consistent with complementary ESEEM studies of the same p21 complex. These studies implicate an oxygen of the β-phosphate and an oxygen of the serine-17 hydroxyl group as direct ligands of the manganous ion but rule out direct coordination by aspartate-57 (Halkides et al., 1994). The overall picture of metal ion coordination, in solution, is broadly consistent with structures determined by X-ray diffraction of *ras* p21·Mg(II)·GDP crystals. The crystal structure of Tong et al., (1991) shows the divalent metal directly coordinated by an oxygen from the β-phosphate and the hydroxyl oxygen of serine-17 with the remaining four ligands presumably water molecules. Schlichting et al. (1990), however, suggested that an oxygen from the carboxyl group of aspartate-57 might also coordinate. The interpretation of Schlichting et al. (1990) implies a hydration number of three and is thus incompatible with the results of this study, the ESEEM studies cited above (Halkides et al., 1994), and the EPR studies by Smithers et al. (1990) and Latwesen et al. (1992).

GTP Form of p21. The application of the spectral subtraction method to EPR signals of H-*ras* p21·Mn(II)·GMPPNP is illustrated in Figure 5. Spectra A and B are EPR signals of p21·Mn(II)·GMPPNP in frozen solutions (with 15% methyl α-D-glucopyranoside) of natural abundance and 30% ^{17}O-enriched water, respectively. Traces C, D, and E are difference spectra calculated by subtracting the various fractions (κ) of spectrum A from spectrum B, with κ equal to 0.70^1, 0.70^2, and 0.70^3 for traces C, D, and E, respectively. The pairs of local extrema appearing in trace C, but not traces D and E, together with calculated difference spectra, lead to the conclusion that the hydration number is two.

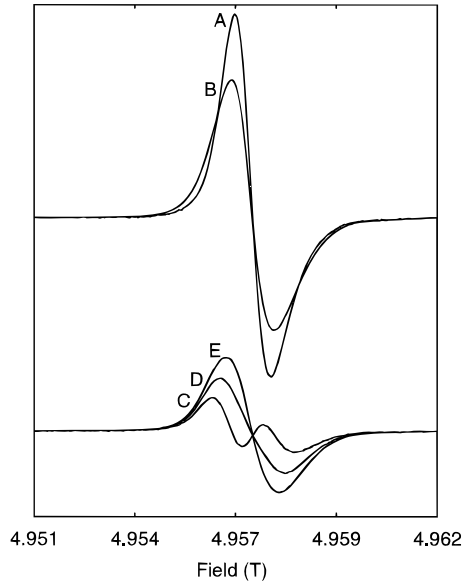

FIGURE 5: (Upper) Overlying EPR spectra of H-*ras* p21·Mn(II)·GMPPNP in frozen solutions with 15% methyl α-D-glucopyranoside and (A) unenriched water and (B) 30% ^{17}O-enriched water. (Lower) Overlying difference spectra calculated with (C) $\kappa = 0.70^1$, (D) $\kappa = 0.70^2$, and (E) $\kappa = 0.70^3$. The pairs of local extrema appearing in (C), but not (D) and (E), indicate that there are two coordination sites for water.

These results represent the first EPR measurement of the hydration number of the divalent metal ion in the GTP form of p21. The result is consistent with the X-ray diffraction-derived binding site structures of p21·Mg(II)·GTP (Schlichting et al., 1990), p21·Mg(II)·GMPPNP (Pai et al., 1990), and p21·Mg(II)·GMPPCP in crystals (Milburn et al., 1990). These crystal structures show the divalent metal ion directly coordinated by the hydroxyl groups of serine-17 and threonine-35, and by the β- and γ-phosphates of GTP or its analogs.

As discussed above, a hydration number of two implies that threonine-35 coordinates directly without an intervening water molecule, consistent with X-ray crystallographic results (Milburn et al., 1990; Pai et al., 1990). Direct coordination of threonine-35 is also consistent with the ESEEM results of (Halkides et al., 1994) provided that the oxygen−manganous ion bond is unusually long (∼2.8 Å). A direct probe of the strength of that interaction is the measurement of the ^{17}O contact hyperfine interaction of the threonine-35 hydroxyl (following paper: Halkides et al., 1996). Here, we demonstrate the feasibility of quantifying ^{17}O hyperfine interactions in the GTP form by high-field EPR spectroscopy: we report here the magnitude of the ^{17}O hyperfine coupling for the two aquo ligands.

The data from which we determine the magnitude of the isotropic ^{17}O hyperfine interaction for the two aquo ligands in H-*ras* p21·Mn(II)·GMPPNP are shown in Figure 6. Spectra A and B (solid) of Figure 6 are EPR signals of p21·Mn(II)·GMPPNP in frozen solutions of natural abundance and 30% ^{17}O-enriched water, respectively. Traces C, D, E, F, G, H, and I (dashed) represent spectrum A after numerical broadening (*vide supra*) by ^{17}O hyperfine coupling constants equal to 0.05, 0.10, 0.15, 0.20, 0.25, 0.30, and 0.35 mT, respectively. The relation of spectrum B to traces G

Table 1: Reported $^{17}O-Mn(II)$ Hyperfine Interactions[a]

sample	label	$\|A_{iso}\|$ (mT)	technique	ref
p21·Mn(II)·GDP	$H_2{}^{17}O$	0.25	EPR	this work
p21·Mn(II)·GMPPNP	$H_2{}^{17}O$	0.28	EPR	this work
$Mn(H_2O)_6{}^{2+}$	$H_2{}^{17}O$	0.27	ENDOR	Glotfelty (1978)
$Mn(H_2O)_6{}^{2+}$	$H_2{}^{17}O$	0.27	ENDOR	Tan (1993)
$MnADP(H_2O)_3{}^{-}$	$H_2{}^{17}O$	0.20	NMR	Zetter et al. (1978)
$Mn(ADP)_2(H_2O)_2{}^{4-}$	$H_2{}^{17}O$	0.25	NMR	Zetter et al. (1978)
CK·Mn(II)·ADP·formate·creatine	[β-^{17}O]ADP	0.3−0.4	EPR	Reed and Leyh (1980)
CK·Mn(II)·ADP·formate·creatine	$HC^{17}O_2{}^{-}$	0.3−0.4	EPR	Reed and Leyh (1980)
EF-Tu·Mn(II)·GDP	[β-$^{17}O_4$]GDP	0.25	EPR	Kalbitzer et al. (1983)
EF-Tu·Mn(II)·GDP·P_i	[β-$^{17}O_4$]GDP	0.16	EPR	Kalbitzer et al. (1984)
AK·Mn(II)·ATP	[β-$^{17}O_4$]ATP	0.22	EPR	Kalbitzer et al. (1983)
AK·Mn(II)·ATP	(R_p)-[β-^{17}O]ATP	0.23	EPR	Kalbitzer et al. (1983)
$p21_c$·Mn(II)·GDP	[β-$^{17}O_4$]GDP	0.16	EPR	Feuerstein et al. (1987)
$p21_v$·Mn(II)·GDP	[β-$^{17}O_4$]GDP	0.22	EPR	Feuerstein et al. (1987)
$p21_t$·Mn(II)·GDP	[β-$^{17}O_4$]GDP	0.16	EPR	Feuerstein et al. (1987)
$p21_{EJ}$·Mn(II)·GDP	[β-$^{17}O_4$]GDP	0.29	EPR	Latwesen et al. (1992)
PK·Mn(II)·oxalate·ATP	[γ-^{17}O]ATP	0.27−0.35	ENDOR	Tan et al. (1993)
PK·Mn(II)·oxalate·ATP	$C_2{}^{17}O_4{}^{2-}$	0.29−0.39	ENDOR	Tan et al. (1993)

[a] Abbreviations: $p21_c$, cellular H-*ras* p21 containing Gly-12 and Ala-59; $p21_t$, T24 mutant form containing Val-12; $p21_v$, viral H-*ras* p21 containing Arg-12 and Thr-59; $p21_{EJ}$, mutant containing Val-12 and Thr-59; AK, adenylate kinase; CK, creatine kinase; PK, pyruvate kinase.

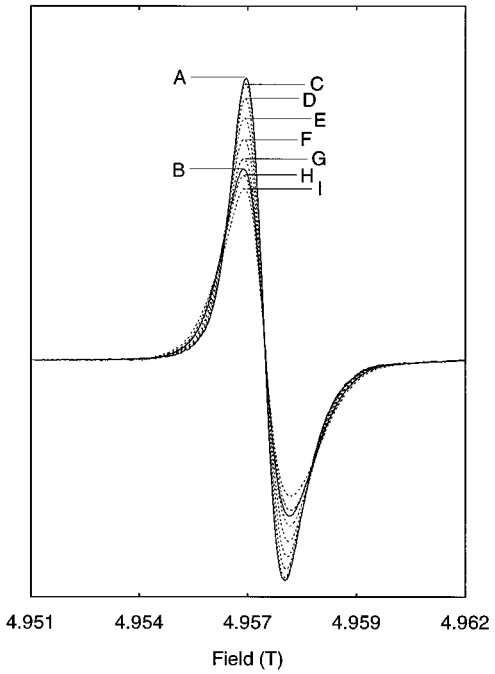

FIGURE 6: The solid traces are the EPR signals of H-*ras* p21·Mn(II)·GMPPNP with 15% methyl α-D-glucopyranoside in (A) unenriched water and (B) 30% ^{17}O-enriched water. The dashed traces represent spectrum A after being broadened by simulated hyperfine interactions with two equivalent aquo ligands of 30% ^{17}O enrichment with ^{17}O hyperfine coupling constants equal to (C) 0.05, (D) 0.10, (E) 0.15, (F) 0.20, (G) 0.25, (H) 0.30, and (I) 0.35 mT.

and H shows graphically that the actual hyperfine coupling constant is between 0.25 and 0.30 mT. Interpolation yields a value of 0.28 mT as the best estimate of the hyperfine coupling constant. We applied an analogous analysis to the GDP complex and obtain a value of 0.25 mT as the best estimate of the average hyperfine coupling constant (data not shown). These values fall within the narrow range of values previously reported for $^{17}O-Mn(II)$ interactions and are shown in Table 1. In particular, the measured coupling constants are in excellent agreement with those determined for $H_2{}^{17}O$, all of which lie between 0.20 and 0.29 mT (Glotfelty, 1978; Tan, 1993; Tan et al., 1993; Zetter et al., 1978). A further discussion of $^{17}O-Mn(II)$ hyperfine coupling constants is presented in the following paper (Halkides et al., 1996).

CONCLUSIONS

In this paper we extend the EPR spectroscopy of *ras* p21 to high frequency. In spectra acquired at 139.5 GHz, in a magnetic field of 4.95 T, the contribution of the second-order fine structure broadening to the width of the central fine structure transition is reduced relative to spectra acquired at low field. High frequency EPR spectroscopy thus enhances sensitivity to ^{17}O hyperfine broadening. The results of this work suggest the feasibility of using high frequency EPR spectroscopy, in conjunction with specific ^{17}O-labeling, to probe Mn(II) systems with larger fine structure interactions, such as the GTP form of EF-Tu (Kalbitzer et al., 1984).

In order to effect meaningful comparisons between these results and those of previous ESEEM studies (Halkides et al., 1994; Halkides et al., submitted for publication), experiments were carried out in frozen solutions containing 15% methyl α-D-glucopyranoside. For a p21·Mn(II)·GDP complex, we have determined a hydration number in frozen solution which is identical to that reported in fluid solution and have demonstrated that the introduction of methyl α-D-glucopyranoside as a cryoprotectant does not affect that hydration number. We have also extended the application of the spectral subtraction method introduced by Reed to dispersion mode spectra. This extension is particularly useful for spectra which have broad lines despite the high magnetic field strengths (*e.g.*, broad lines resulting from insufficient cyroprotection) and for which absorption mode spectra yield equivocal results.

We have determined the number of water molecules coordinating manganese in frozen solutions of N-*ras* p21-GDP and H-*ras* p21-GTP to be four and two, respectively. These results imply that threonine-35 is a ligand of the divalent metal ion in the GTP complex, as is suggested by X-ray crystallography-derived binding site structures, and resolve a question raised by recent ESEEM studies (Halkides et al., 1994). In light of the ESEEM work, we infer that this coordination, although direct, must be weak. A critical test of this conjecture is the measurement of the ^{17}O contact hyperfine interaction for the hydroxyl group of threonine-

35, presented in the following paper (Halkides et al., 1996). To demonstrate the feasibility of our experimental protocol, we have made the analogous measurement for the aquo ligands in p21·Mn(II)·GMPPNP and p21·Mn(II)·GDP and found the average magnitude of the ^{17}O hyperfine interaction to be 0.28 and 0.25 mT, respectively. These values are consistent with measurements made in a variety of ^{17}O−Mn(II) systems.

ACKNOWLEDGMENT

We thank Professor George H. Reed for determining the value of the zero-field splitting parameter of p21·Mn(II)·GMPPNP. We thank Dr. Frank McCormick and co-workers for the gift of *ptrc* bearing the N-*ras* gene and Professor Lawrence Feig for the gift of plasmid pXVR bearing the H-*ras* gene. We gratefully acknowledge Professor Alfred G. Redfield for his support and helpful comments.

REFERENCES

Abragam, A., & Bleaney, B. (1970) *Electron Paramagnetic Resonance of Transition Ions*, Dover, New York.
Barbacid, M. (1987) *Annu. Rev. Biochem. 56*, 779−827.
Becerra, L. R., Gerfen, G. J., Bellew, B. F., Bryant, J. A., Hall, D. A., Inati, S. I., Weber, R. T., Un, S., Prisner, T. F., McDermott, A. E., Fishbein, K. W., Kreischer, K. E., Temkin, R. J., Singel, D. J., & Griffin, R. G. (1995) *J. Magn. Reson., Ser. A 117*, 28−40.
Bourne, H. R., Sanders, D. A., & McCormick, F. (1990) *Nature 348*, 125−132.
Bourne, H. R., Sanders, D. A., & McCormick, F. (1991) *Nature 349*, 117−127.
Buchbinder, J. L., & Reed, G. H. (1990) *Biochemistry 29*, 1799−1806.
Downward, J. (1990) *Trends Biochem. Sci. 15*, 469−472.
Feuerstein, J., Kalbitzer, H. R., John, J., Goody, R. S., & Wittinghofer, A. (1987) *Eur. J. Biochem. 162*, 49−55.
Foley, C. K., Pedersen, P. S., Charifson, T. A., Darden, T. A., Wittinghofer, A., Pai, E. F., & Anderson, M. W. (1992) *Biochemistry 31*, 4951−4959.
Glotfelty, H. W. (1978) Ph.D. Thesis, University of Kansas.
Halkides, C. J., Farrar, C. T., Larsen, R. G., Redfield, A. G., & Singel, D. J. (1994) *Biochemistry 33*, 4019−4035.
Halkides, C. J., Bellew, B. F., Gerfen, G. J., Farrar, C. T., Carter, P. H., Ruo, B., Evans, D. A., Griffin, R. G., & Singel, D. J. (1996) *Biochemistry 35*, 12194−12200.
Kalbitzer, H. R., Marquetant, R., Connolly, B. A., & Goody, R. S. (1983) *Eur. J. Biochem. 133*, 221−227.
Kalbitzer, H. R., Goody, R. S., & Wittinghofer, A. (1984) *Eur. J. Biochem. 141*, 591−597.
Kofron, J. L., Ash, D. E., & Reed, G. H. (1992) *Biochemistry 27*, 4781−4787.
Larsen, R. G., Halkides, C. J., Redfield, A. G., & Singel, D. J. (1992) *J. Am. Chem. Soc. 114*, 9608−9611.
Latwesen, D. G., Poe, M., Leigh, J. S., & Reed, G. H. (1992) *Biochemistry 31*, 9608−9611.
Leyh, T. S., Sammons, R. D., Frey, P. A., & Reed, G. H. (1982) *J. Biol. Chem. 257*, 15047−15053.
Lodato, D. T., & Reed, G. H. (1987) *Biochemistry 26*, 2243−2250.
Marshall, M. S. (1993) *Trends Biochem. Sci. 18*, 250−254.
Milburn, M., Tong, L., DeVos, A. M., Brunger, A., Yamaizumi, Z., Nishimura, S., & Kim, S.-H. (1990) *Science 247*, 939−945.
Moodie, S. A., Willumsen, B. M., Weber, M. J., & Wolfman, A. (1993) *Science 260*, 1658−1661.
Moore, J. M., & Reed, G. H. (1985) *Biochemistry 24*, 5328−5333.
Olsen, L. R., & Reed, G. H. (1993) *Arch. Biochem. Biophys. 304*, 242−247.
Pai, E. F., Krengel, U., Petsko, G., Goody, R. S., Kabsch, W., & Wittinghofer, A. (1990) *EMBO J. 9*, 2351−2359.
Prisner, T. F., Un, S., & Griffin, R. G. (1992) *Isr. J. Chem. 32*, 357−363.
Reed, G. H., & Leyh, T. S. (1980) *Biochemistry 19*, 5472−5480.
Reed, G. H., & Markham, G. D. (1984) *Biol. Magn. Reson. 6*, 73−142.
Schlichting, I., Almo, S. C., Rapp, G., Wilson, K., Petratos, K., Lentfer, A., Wittinghofer, A., Kabsch, W., Pai, E. F., Petsko, G. A., & Goody, R. (1990) *Nature 345*, 309−315.
Shirouzu, M., Koide, H., Fujita-Yoshigaki, J., Oshio, H., Toyama, Y., Yamasaki, K., Fuhrman, S. A., Villafranca, E., Kaziro, Y., & Yokoyama, S. (1994) *Oncogene 9*, 2153−2157.
Smithers, G. W., Poe, M., Latwesen, D. G., & Reed, G. H. (1990) *Arch. Biochem. Biophys. 280*, 416−420.
Tan, X. (1993) Ph.D. Thesis, State University of New York at Albany.
Tan, X., Poyner, R., Reed, G. H., & Scholes, C. P. (1993) *Biochemistry 32*, 7799−7810.
Tan, X., Bernardo, M., Thomann, H., & Scholes, C. P. (1995) *J. Chem. Phys. 102*, 2675−2689.
Tong, L., deVos, A. M., Milburn, M. V., Brunger, A., & Kim, S.-H. (1991) *J. Mol. Biol. 217*, 503−516.
Un, S., Bryant, J. A., & Griffin, R. G. (1989) *J. Magn. Reson. 101*, 92−104.
Wittinghofer, A., Goody, R. S., Rosch, P., & Kalbitzer, H. R. (1982) *Eur. J. Biochem. 124*, 109−115.
Zetter, M. S., Lo, G. Y.-S., Dodgen, H. W., & Hunt, J. P. (1978) *J. Am. Chem. Soc. 100*, 4430−4436.

BI960594B